INFLUENCE OF VOLUMETRIC RADIATION PROPERTIES ON NATURAL CONVECTION IN THE LOW MACH NUMBER APPROXIMATION

Nesrine RACHEDI[1], Messaoud GUELLAL[1*] and Madiha BOUAFIA[2]

[1]Laboratory of Chemical Process Engineering, University of Sétif 1 - Ferhat ABBAS, Algeria

[2]Laboratory of Mechanics and Energetics of Evry, University of Evry Val d'Essonne, France

*Corresponding author; E-mail: mguellal@univ-setif.dz

Abstract:

The study aims to investigate the dynamics of fluid flow and thermal energy exchange within a 2D differentially heated cavity using the low Mach number approximation. Specifically, it seeks to investigate the occurrences related to natural convection and thermal radiation in a medium that exhibits absorption, emission, and scattering properties and exposed to a significant temperature difference. This methodology is applied within the framework of the low Mach number model of the Navier-Stokes equation. The interaction of momentum, energy, and radiation transfer equations within the cavity is addressed through an iterative approach that combines discrete-ordinates and finite volume methods enhanced by the SIMPLER algorithm. The obtained findings show that the LMN model overestimates radiative transfer, with higher radiative power in the absorbing-emitting case. Transparent media ($\tau = 5$) result in the highest heat transfer, while lower opacity favors the absorbing-diffusing medium. Flow intensity increases with albedo, and isotherms deform due to strong fluid dynamics. At high opacity, heat transfer is greater in transparent media, with lower velocities in more diffusing media.

Keywords: Transparency, Absorbing-emitting-scattering, Coupling, Convection, Radiation, Rayleigh, Opacity, Planck.

1. Introduction

The transfer of thermal energy within a system is a fundamental aspect of heat transfer analysis, encompassing convection, conduction, and radiation. Traditionally, convection and radiation have been treated as distinct processes; however, in reality, they are closely intertwined, and their interactions can significantly impact the thermal dynamics of a system. Understanding this coupling is crucial in numerous engineering domains, especially in scenarios requiring accurate heat transfer forecasts, such as in high-temperature furnaces, solar energy systems, rocket propulsion, and industrial heating processes [1, 10, 14].

Participating media, which can absorb, emit, and scatter thermal radiation, play a crucial role in fields such as solar energy harvesting, medical technology, chemical processing, and aerospace engineering [11, 12]. The challenge in these domains lies in addressing the varying scales of thermal processes and the distinct contributions of convection and radiation. At elevated temperatures, radiative heat transfer assumes dominance, while at lower temperatures, it plays a minor role unless stimulated by an external radiation source. In non-participating media, heat transfer primarily hinges on conduction and convection, both of which exhibit linearity concerning temperature gradients. In contrast, radiative heat transfer is contingent on the fourth power of temperature, rendering it the predominant mechanism in high-temperature environments.

Radiative transfer is mathematically represented by the Radiative Transfer Equation (RTE), an integro-differential equation that accounts for the spatial and angular variations in radiation intensity. Solving the RTE is computationally complex and requires sophisticated numerical methods. The Discrete Ordinates Method (DOM), when combined with finite volume formulations, is frequently employed due to its ability to integrate radiation with the governing equations of fluid flow and energy transfer. This integration enables a more comprehensive analysis of heat transfer by concurrently solving the RTE and the convection equations on the same computational grid.

Previous studies emphasize the importance of incorporating realistic fluid properties, significant temperature variations, and the effects of compressibility in thermal models. The Low Mach Number (LMN) approximation, derived from compressible Navier-Stokes equations, is particularly useful for modeling low-velocity compressible flows. This approach simplifies computations by separating pressure into a uniform thermodynamic component and a dynamic component. By removing acoustic waves from the equations, the LMN approximation allows for larger time steps in numerical simulations while still accounting for density changes caused by temperature variations.

The interaction between radiation and convection in participating media is further influenced by boundary conditions and the interaction between solids and fluids. This study adopts the LMN approximation to tackle these complexities and to simulate the combined effects of natural convection and radiation in a two-dimensional cavity. Through examining the roles of radiative properties and fluid characteristics, this work aims to deepen the understanding of coupled heat transfer processes in engineering systems.

The differential heating of cavities is a well-known problem often utilized to validate computational fluid dynamics (CFD) codes. To our knowledge, the publications of Lauriat [1], Yucel et al. [2], Draoui et al. [3], Fusegi and Farouk [4] and Tan and Howel [5] are among the first published works dealing with the problem of radiation / convection coupling in semi-transparent medium. In most of the works, authors have demonstrated the significant and at times predominant role of radiation in heat transfers. However, the influences of the types of boundary conditions and the geometrical configuration on the flow stability and the heat exchange coefficients are generally rarely studied, though they are of great importance. As a fact of matter, it is useful for a practitioner to know, for a given geometry, the condition types at boundaries or which geometrical configuration allows obtaining, for example, the desired heat transfer coefficient.

From a fundamental viewpoint, in these kinds of problems, the combined study of their influences and of the radiation can provide valuable information on flow stability, regime transition, etc. The interaction of radiation with a material medium (solid, liquid, gas) gives rise to four kinds of phenomena: emission, adsorption, diffusion (gas, particles), reflection / refraction. These phenomena are linked to the atomic and molecular characteristics of the crossed medium and to the macroscopic (geometrical) or physical (conductivity) characteristics of the material. In recent years, there has been an increasing emphasis on numerical studies concerning the flows of radiating fluids confined within cavities. The commonly encountered configuration involves a differentially heated cavity, where two vertically opposing walls are kept at constant temperatures, whereas the other walls are adiabatic and horizontally oriented. The authors often consider the flow of radiating grey fluids in two-dimensional cavities in steady state [1, 2, 5].

These studies have demonstrated that under convective conditions, radiation increases the flow velocity and reduces vertical thermal stratification. Borjini et al. [6] in their investigation of grey fluids in a square cavity, found that radiative transfers accentuate three-dimensional effects at intermediate optical thicknesses. Furthermore, the grey gas approximation tends to overestimate radiative transfers and fails to accurately predict velocity and temperature fields [7, 8]. The substantial computational resources required for unsteady numerical simulations have remained a limiting factor in exploring transitional regimes of turbulent radiative gases. Existing research predominantly employs Reynolds-averaged simulations [4] or computationally intensive simulations [9].

Moufekkir et al. [10] studied how radiation affects natural convection heat transfer in a square enclosure filled with a gas that interacts with radiation under typical conditions. The results show that radiation enhances temperature and velocity gradients, while a scattering medium generates multicellular flow dynamics. Similarly, Xianglongliu et al. [11] developed a computer model that replicates natural convection combined with volume radiation in a two-dimensional square cavity, including an absorbing, emitting, and diffusing medium. This study demonstrated that heat transfer is influenced by the medium's properties and cavity geometry, with natural convection enhancing heat fluxes while altering Nusselt number distributions. Mezrab et al. [12] provided computational solutions for the interaction between radiation and natural convection heat transfer by implementing double diffusion within a square enclosure filled with an absorbing, emitting, and non-diffusing grey gas. The provided results serve as a benchmark solution. Their results, serving as a benchmark for further studies, reveal that radiation increases fluid temperature, enhances the thermal gradient on the cold wall, and reduces it on the hot wall, thereby accelerating flow velocity. In double-diffusive flows, the impact of radiation is influenced by parameters such as flow type, buoyancy ratio (N), and Rayleigh number (Ra). Ki Hong Byun et al. [13] investigated the role of wall specular reflection on natural convection heat transfer combined with radiation in an infinitely long square pipe filled with a grey medium capable of absorbing and emitting radiation. Their findings emphasize the Rayleigh number, conduction-to-radiation ratio, and wall emissivity are crucial in determining heat transfer and fluid flow behavior. Specifically, lower conduction-to-radiation ratios and reduced wall emissivity lead to more pronounced variations in heat flux and temperature distributions, with specular reflection significantly influencing fluid motion. Chaabane et al. [14] introduced an innovative computational approach to analyze the interaction between natural convection and radiation in a two-dimensional enclosure containing a medium capable of absorbing, emitting, and diffusing radiation. They solved the radiative transfer equation using the control volume finite element method (CVFEM) and computed density, velocity, and temperature variables with the Lattice Boltzmann equation (LBE) utilizing two double populations. The results, validated against existing studies, demonstrated that the proposed method is both efficient and accurate, with good numerical stability. Other authors interested in heat transfer in transparent media have explored the surface radiation's impact on free convection in confined cavities [15-17]. Wang et al. [15] developed a numerical model

to study the interaction of natural convection and surface radiation in a square cavity filled with air. Their results show that surface radiation reduces thermal stratification, cools the top wall, and heats the bottom wall, while increasing airflow along the horizontal walls. They also found that at low Rayleigh numbers, radiative heat flux is proportional to the temperature difference, and radiation induces earlier time-dependent flows with multiple periodic solutions within a specific Rayleigh number range. Hamimid et al. [16] explored natural convection and surface radiation in a square enclosure using a low Mach-number model. The study found that temperature differences and surface emissivity greatly influence heat transfer and fluid flow, with radiation reducing thermal stratification and enhancing horizontal flow. Bouafia et al. [17] investigated the effect of surface radiation on natural convection in a square cavity with large temperature differences using numerical simulations. They found that radiation alters heat transfer by cooling the top wall and heating the bottom wall, while reducing thermal stratification.

Kogawa et al. [18] investigated the impact of thermal radiation on turbulence in natural convection, revealing that radiation can either enhance or suppress turbulence depending on the absorption coefficient. They observed that radiation thickens the thermal boundary layer, stabilizing the flow by reducing instabilities. Parsaee et al. [19] studied the effects of a variable radiative absorption coefficient on heat transfer in a magnetized fluid-filled cavity. Their results showed that using a variable coefficient reduced heat transfer by 10.5%, with the effect varying based on the Hartmann and Rayleigh numbers. Barbosa et al. [20] explored heat transfer in square enclosures containing CO_2 , emphasizing the influence of radiation and geometric factors. Radiation increased heat transfer by up to fourfold, while protrusions improved temperature distribution and airflow, enhancing overall efficiency. Sertel et al. [21] examined the interaction of convective and radiative heat transfer in tube banks within a participating medium. They found that medium properties, such as scattering and tube spacing, significantly influenced heat transfer and developed a highly accurate correlation for predicting Nusselt numbers. Moutahir et al. [22] developed mathematical models to simulate radiative and conductive heat transfer in non-grey media undergoing phase changes. Their study highlighted the critical role of thermal radiation in accurately predicting phase transitions and interface dynamics in high-temperature processes.

In our previous study, we utilized the Boussinesq approximation to explore numerically the interplay of natural convection and radiation within a square cavity containing a grey non-diffusing and semi-transparent fluid [23]. The present investigation seeks to build upon previous research by exploring a medium that both absorbs and emits light while also diffusing it. This study aims to accurately model the coupling effects of convection and radiation in heat transfer problems. The applied conditions are designed to reproduce realistic scenarios in high-temperature applications, such as solar collectors and heating furnaces, where radiation often dominates heat transfer due to its dependence on the fourth power of absolute temperature. Considering these conditions, the study highlights the inherent coupling between convection and radiation, especially in the participating media, allowing a comprehensive understanding of their interactions. The use of the discrete ordinate method (DOM) facilitates numerical solvability and model validation, addressing the challenges posed by high-temperature environments and compressibility effects. Furthermore, the use of the low Mach number (LMN) approximation ensures computational efficiency by simplifying the treatment of density fluctuations with temperature. The research offers a robust framework for exploring various engineering applications.

2. Mathematical formulation

We consider a Newtonian fluid with a presumed laminar and steady flow, governed by the Navier-Stokes equations obtained under the assumption of the low Mach number. An ideal gas equation of state is adopted, and the transport equations are solved in a conservative manner. The low Mach number approximation accounts for the density dependence on temperature everywhere in the governing transport equations, while in the Boussinesq approximation the connection between the temperature field and the dynamic one is only obtained through the buoyancy term. The radiative transfer equation (RTE) is solved using the discrete ordinate method (DOM) for an absorbing, emitting, and isotropically scattering gray gas, thus determining the intensity field of the radiation [24].

A source component is included in the energy equation to ensure the coupling of radiation and convection in situations involving a participating medium. Figure 1 illustrates the suggested physical model. The cavity is a square containing a perfect, compressible gas under the influence of a gravitational field parallel to the vertical walls. The walls on the left and right sides have constant temperatures, T_C and T_H respectively, where T_H is greater than T_C. The horizontal walls are designed to be adiabatic. Each wall is considered dark and diffusely reflecting.

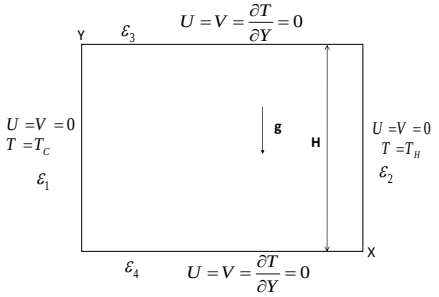

Figure 1. Non-dimensional radiative heat flux on the hot wall

Under these assumptions, the governing equation may be written in a dimensionless manner as follows [16, 17, 26]:

$$\frac{\partial \rho}{\partial t} + \frac{\partial \rho U}{\partial X} + \frac{\partial \rho V}{\partial Y} = 0 \tag{1}$$

$$\rho\left(\frac{\partial U}{\partial t} + U\frac{\partial U}{\partial X} + V\frac{\partial U}{\partial Y}\right) = -\frac{\partial \pi}{\partial X} + Pr\left(\frac{\partial}{\partial X}\left(\mu\frac{\partial U}{\partial X}\right) + \frac{\partial}{\partial Y}\left(\mu\frac{\partial U}{\partial Y}\right) + \frac{1}{3}\nabla\mu\nabla\vec{V}\right) \tag{2}$$

$$\rho\left(\frac{\partial V}{\partial t} + U\frac{\partial V}{\partial X} + V\frac{\partial V}{\partial Y}\right) = -\frac{\partial \pi}{\partial Y} - RaPr\frac{\rho-1}{2\varepsilon_b} + Pr\left(\frac{\partial}{\partial X}\left(\mu\frac{\partial V}{\partial X}\right) + \frac{\partial}{\partial Y}\left(\mu\frac{\partial V}{\partial Y}\right) + \frac{1}{3}\nabla\mu\nabla\vec{V}\right) \tag{3}$$

$$\rho C_P\left(\frac{\partial T}{\partial t} + U\frac{\partial T}{\partial X} + V\frac{\partial T}{\partial Y}\right) = \frac{\partial}{\partial X}\left(k\frac{\partial T}{\partial X}\right) + \frac{\partial}{\partial Y}\left(k\frac{\partial T}{\partial Y}\right) + \frac{\gamma-1}{2\varepsilon_b\gamma}\frac{d\bar{P}}{dt} - \nabla.\vec{Q}_r \tag{4}$$

$$\rho = \frac{\bar{P}}{(2\varepsilon_b T+1)} \tag{5}$$

The rate of radiative exchange in the energy balance of the cavity is determined by the source term of the energy equation, which is equivalent to the divergence of the radiative flow. This term is calculated by solving the radiative transfer equation, which is written in Cartesian coordinates for a two-dimensional medium with scattering properties [24]:

$$\xi\left(\frac{\partial L}{\partial X}\right) + \eta\left(\frac{\partial L}{\partial Y}\right) + \tau L = \frac{\tau}{\pi}\left[(1-\omega)(1+2\varepsilon_b T)^4 + \omega\int_{4\pi} L d\Omega\right] \tag{6}$$

The flux divergence may be determined by using the solution to equation (6) in the following manner:

$$\nabla\overrightarrow{Q_r} = \frac{(1-\omega)\tau}{Pl}\left[4(1+2\varepsilon_b T)^4 - \int_{4\pi} L\, d\Omega\right]$$

The discretization of the radiative transfer equation is conducted for a particular direction Ω_m and then resolved using the finite volume method [25]:

$$\xi_m\frac{\partial L_m}{\partial X} + \eta_m\frac{\partial L_m}{\partial Y} + \tau L_m = \tau L_b \tag{7}$$

With :

$$L_b = \frac{1}{\pi}\left[(1-\omega)(1+2\varepsilon_b T)^4 + \omega\int_{4\pi} L d\Omega\right]$$

By integrating equation (7) of the radiative transfer equation over the control volume results in:

$$\xi_m A_y\left(L_{m,E} - L_{m,W}\right) + \eta_m A_x\left(L_{m,N} - L_{m,S}\right) + \tau\Delta V L_{m,P} = \tau\Delta V L_b \tag{8}$$

With: $A_x = \Delta X$, $A_y = \Delta Y$ and $\Delta V = \Delta X\Delta Y$

ξ_m and η_m mare are the positive direction cosines according to X and Y.
$L_{m,P}$ signifies the luminance value at the center, while $L_{m,E}$, $L_{m,W}$, $L_{m,N}$, and $L_{m,S}$ denote the luminance values in the corresponding East, West, North, and South directions.

The luminance values are known on the West and South faces, while they are unknown at the center (P) and on the East and North faces. We therefore need two additional relationships. Through interpolation, the unknown

luminances L_E and L_N are removed, leading to equation (7) being simplified into an explicit relationship between the unknown luminance L_P and the known luminances L_W, L_S, and L_b.

$$L_P = \frac{\lambda_x L_W + \lambda_y L_S + \tau \Delta V L_b}{\lambda_x + \lambda_y + \tau \Delta V} \quad (9)$$

With: $\lambda_x = \frac{\xi_m A_y}{a}$ and $\lambda_y = \frac{\eta_m A_x}{b}$

In a diamond system, a = b = 0.5, while a = b = 1 indicates the step scheme.

The Step method is applied to the algebraic equations derived from Equation (8). The relationship between natural convection and radiation of the cavity's participating medium is resolved via an iterative process. The RTE equation coupling influences heat flows by altering the local temperature of the medium after the RTE is solved:

$$-\frac{\partial T}{\partial Y} = \frac{\varepsilon_3}{Pl}[Q_{inc} - (1 + 2\varepsilon_b T)^4] \text{ at } Y = 0 \text{ and } 0 \le X \le 1 \quad (10)$$

$$+\frac{\partial T}{\partial Y} = \frac{\varepsilon_4}{Pl}[Q_{inc} - (1 + 2\varepsilon_b T)^4] \text{ at } Y = 1 \text{ and } 0 \le X \le 1 \quad (11)$$

We calculate Q_{inc} from:

$$Q_{inc}(X, 0) = \sum_{\xi_m < 0} |\eta_m| \, \omega_m \, L(X, 0) \quad (12)$$

$$Q_{inc}(X, 1) = \sum_{\xi_m > 0} |\eta_m| \, \omega_m \, L(X, 1) \quad (13)$$

The temperature boundary conditions are as follows:

$$T = T_C \text{ at } X = 0 \text{ and } 0 \le Y \le 1 \quad (14)$$

$$T = T_H \text{ at } X = 1 \text{ and } 0 \le Y \le 1 \quad (15)$$

In radiative heat transfer, the boundary conditions of a problem are typically represented by a locally flat, opaque surface that participates in radiative exchanges. For a gray, opaque, and diffuse surface, the radiance at the boundary consists of two main contributions [24]:
-The radiance emitted by the boundary itself;
- The incident radiance from the medium, which is partially reflected by the surface.

The radiative intensity is given by the equation:

$$L_\lambda(s_p, \vec{S}) = \varepsilon_p L_{b,\lambda}(T_p) + (1 - \varepsilon_p)\frac{q_\lambda^{inc}(s_p)}{\pi} \quad (16)$$

This condition applies to all directions such that $\vec{S}.\overrightarrow{n_p} > 0$, where $\overrightarrow{n_p}$ is the surface normal vector pointing inward into the domain.

Where:

ε_p: emissivity of the surface;

T_p: local surface temperature;

$q_\lambda^{inc}(s_p)$: incident radiative flux density on the surface at the specified point.

The incident radiative flux density, $q_\lambda^{inc}(s_p)$, is determined by:

$$q_\lambda^{inc}(s_p) = \int_{\overrightarrow{n_p}.\overrightarrow{s'}<0}^{0} L_\lambda(s_p, \overrightarrow{S'}) \left|\overrightarrow{n_p}.\overrightarrow{S'}\right| d\Omega' \; \overrightarrow{n_p}.\vec{S} > 0$$

Here:

$\overrightarrow{S'}$ represents the direction of the incident radiation on the surface;

$d\Omega'$ is the elemental solid angle around the direction $\overrightarrow{S'}$.

The radiation boundary conditions are:

$$L(X, 0) = \frac{\varepsilon_4}{\pi}(1 + 2\varepsilon_b T(X, 0))^4 + \frac{1 - \varepsilon_4}{\pi} Q_{inc}(X, 0) \text{at} \quad Y = 0 \quad \text{for} \quad \eta_m < 0 \quad (17)$$

$$L(X, 1) = \frac{\varepsilon_3}{\pi}(1 + 2\varepsilon_b T(X, 1))^4 + \frac{1 - \varepsilon_3}{\pi} Q_{inc}(X, 1) \text{at} \quad Y = 1 \quad \text{for} \quad \eta_m > 0 \quad (18)$$

$$L(0,Y) = \frac{\varepsilon_1}{\pi}(1 + 2\varepsilon_b T(0,Y))^4 + \frac{1-\varepsilon_1}{\pi} Q_{inc}(0,Y) \text{at} \quad X = 0 \quad \text{for} \quad \xi_m < 0 \tag{19}$$

$$L(1,Y) = \frac{\varepsilon_2}{\pi}(1 + 2\varepsilon_b T(1,Y))^4 + \frac{1-\varepsilon_2}{\pi} Q_{inc}(1,Y) \text{ at} \quad X = 1 \quad \text{for} \quad \xi_m > 0 \tag{20}$$

3. Thermal transfer variables

The average Nusselt numbers quantify the effects of heat convection and radiation over the active walls, as specified by [24, 25, 27]:

$$Nu_{CV} = \int_0^1 \frac{-k}{2\varepsilon_b} \left|\frac{\partial T}{\partial X}\right|_{X=0,1} dY \tag{21}$$

$$Nu_R = \frac{1}{2\varepsilon_b Pl} \int_0^1 |Q_{rnet}|_{X=0,1}\, dY \tag{22}$$

The average total Nusselt number is a specified quantity:

$$Nu_T = Nu_{CV} + Nu_R \tag{23}$$

4. Numerical method

To solve the governing differential equations for velocity, pressure, and temperature fields, the finite volume technique is utilized. To estimate the advection-diffusion terms, a power scheme is employed. The coupling between pressure and velocity is resolved using the SIMPLER algorithm (Semi-Implicit Method for Pressure Linked Equations Revised) with a staggered grid, as described in Patankar [26]. The equations governing the system are formulated in a transient form, and to achieve a steady state solution, an iterative procedure utilizing a fully implicit transient differencing scheme is implemented. The line-by-line Thomas algorithm is utilized to solve the discretized equations, incorporating two directional sweeps (Figure 2).

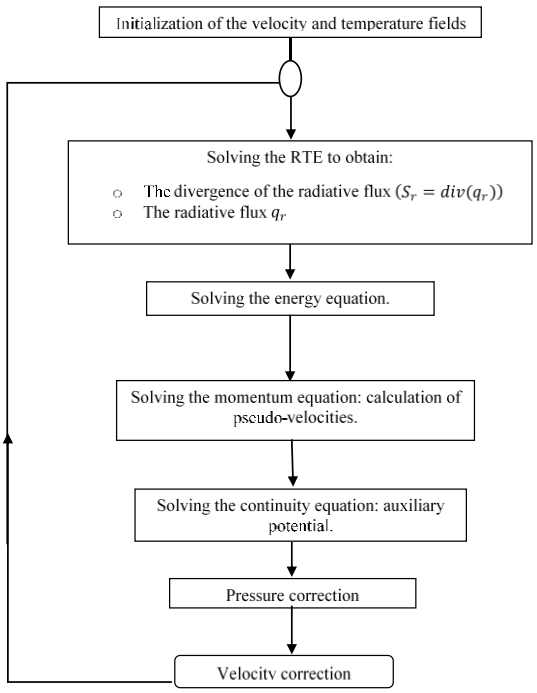

Figure 2: Numerical Algorithm

In this study, a grid with dimensions of 150 x 150 points is selected to strike a balance between the required accuracy and computational time. To ensure satisfactory convergence of the solutions, a convergence criterion of 10^{-5} is set for the residuals. The outer iterative loop continues until a steady state is reached, which is determined by the simultaneous satisfaction of the following convergences: $\left|\phi_{ij}^{old} - \phi_{ij}\right| \leq \varepsilon_\phi$, where ϕ represents the variables U, V, or T. To calculate the source term in Equation 4, which corresponds to the radiative flux, the intensity field is solved using the Radiative Transfer Equation (RTE). The angular discretization is performed using the discrete ordinates method (DOM), as described in [27], with the implementation of an Sn8 quadrature derived from Modest [24]. The Sn8 quadrature is employed to solve radiative transfer equations by discretizing

the angular domain into eight directions. The finite volume approach is employed to discretize the spatial domain. The criteria for convergence in the RTE calculations and for achieving steady state in the remaining governing equations were specified as:

$$Max\left|\frac{L_P^n - L_P^{n-1}}{L_P^n}\right| \leq 10^{-6} \quad \text{and} \quad Max\left|\frac{\phi_P^n - \phi_P^{n-1}}{\phi_P^n}\right| \leq 10^{-6}$$, Where ϕ can be U, V, and T.

5. Mesh sensitivity

Table 1 presents the results for a Rayleigh number of Ra = 5×10^6 and an optical thickness coefficient of τ = 1. The analysis indicates that using finer meshes enhances the accuracy of the results, especially for the average Nusselt number. With a non-uniform mesh of 150×150 nodes, the maximum deviation observed is just 0.79%. Furthermore, both the total and radiative Nusselt numbers (Nu_T and Nu_R) show stable values with the 150×150 mesh, and no significant changes are observed with even finer meshes. This mesh size is sufficient to obtain accurate results while optimizing computational efficiency.

Table 1: Radiative and total averaged Nusselt number for Ra = 5×10^6, Pr = 0.71 and τ = 1.

Mesh	80 × 80	100 × 100	150 × 150	200 × 200	250 × 250
Nu_T	39.01	38.70	38.55	38.55	38.55
Nu_R	31.80	31.60	31.37	31.37	31.37

6. Verification

This study is prompted by the lack of experimental and numerical data concerning the integration of natural convection in participating environments under non-Boussinesq conditions. The literature provides limited data on the interactions between compressible convection and volume radiation. To address this gap, we conducted two validation cases. In the first validation test, we performed calculations for a square cavity considering pure radiation conditions. The chosen conditions were similar to those employed by Razzaque et al. [28]. The problem is represented as radiation emitted from surfaces at a temperature of T = 1 K. The top wall is maintained at a specific temperature, with the remaining walls held at 0 Kelvin. We study the radiative equilibrium of the medium by using uniform meshes. Figure 3 evaluates the non-dimensional radiative heat transfer on the heated wall. An increase in the absorption coefficient (κ) results in more energy emission from the substance. As a result, the net heat flow Q_r decreases, but the radiated power from the hot wall stays constant. The comparison reveals a satisfactory degree of concordance among the findings.

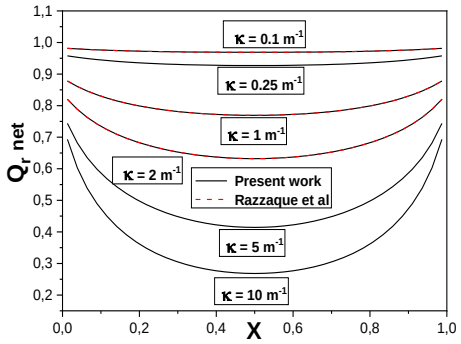

Figure 3. Non-dimensional radiative heat flux on the hot wall

The code developed in this study underwent a secondary validation to verify its precision in modeling the interaction between natural convection and volumetric radiation under the Boussinesq approximation. The fluid in question is treated as radiatively grey, with a Prandtl number of 0.71 and a Rayleigh number of 5×10^6. To evaluate the impact of radiative transfer, simulations were performed for multiple optical thickness values (τ = 0.2, 1, 5). The cavity walls were assumed perfectly black, simplifying the boundary conditions by considering ideal emissivity. The simulation results demonstrate strong alignment with previously published data, as illustrated in Table 2, with a maximum observed deviation of just 2.281%. This minimal variation highlights the effectiveness and accuracy of the implemented model in capturing the combined effects of natural convection and volumetric radiation across different optical regimes.

Table 2. Radiative and global average Nusselt values on the heated wall of the cavity.

τ	Present work		Yucel **[2]**		Laouar-Meftah **[29]**		Moufekkir et al. **[10]**	
	Nu_T	Nu_r	Nu_T	Nu_r	Nu_T	Nu_r	Nu_T	Nu_r
0.2	46.395	38.07	46.39 (0.10%)	37.39 (1.78%)	46.05 (0.74%)	37.4 (1.75%)	45.509 (1.94%)	36.718 (3.55%)
1	38.55	31.37	39.45 (2.28%)	31.77 (1.27%)	38.81 (0.66%)	31.25 (0.38%)	38.725 (0.45%)	31.108 (0.83%)
5	31.84	23.61	32.06 (0.68%)	23.96 (1.48%)	31.59 (0.79%)	23.57 (0.16%)	31.778 (0.19%)	23.801 (0.80%)

7. Results and Discussion

The results relate to the study of grey gas participation effect on the natural convection in a square cavity whose both vertical walls are differentially heated and containing an absorbing, emitting and diffusing medium. In order to investigate the impact of radiative parameters, specifically albedo and optical thickness, on the flow pattern and spatial temperature variation, the following simulation parameters are taken into account: $\varepsilon_b = 0.6$, ($\tau = 0.2, 1, 5$), ($\omega = 0 - 0.75$), $Pr = 0.71$, $Ra = 5.10^6$ and $Pl = 0.02$.

The study carried out is characterized by the graphic visualization of Streamlines contours, the isotherms, the velocity profiles according to X and Y and temperature profiles as a function of the variation in optical thickness for the three cases studied. The different cases studied are reported in table 3.

Table 3. Configurations tested

	Configuration 1	Configuration 2	Configuration 3
Isothermal walls	$\varepsilon = 1$	$\varepsilon = 1$	$\varepsilon = 1$
Adiabatic walls	$\varepsilon = 1$	$\varepsilon = 1$	$\varepsilon = 1$
medium	Transparent $\tau = 0$ et $\omega = 0$	Absorbing and emitting $\tau \neq 0$ et $\omega = 0$	Absorbing and diffusing $\tau \neq 0$ et $\omega \neq 0$

The temperature contours, flow lines, and thermal distributions at mid-planes located at X=0.5 and Y=0.5 are shown in **figures 4 to 6** for each of the studied cases. **Figures 4 and 5** show that isotherms and streamlines of case 3 (absorbing and diffusing) are not greatly influenced by the coefficient of diffusion. There is only a minor decrease in the flow pattern (an increase in ψ_{max}) in the enclosure as ω approaches 1, which corresponds to case 1 (transparent). Additionally, we observe that the gas participation provokes a strengthening of the temperature gradient and of the velocity in proximity to the active walls. In the case of participating medium, we observe a significant alteration in the temperature distribution as the optical thickness rises. We notice also a temperature homogenization in the cavity. When considering the absorbing and diffusing gas, it is evident that the fluid motion experiences a notable acceleration, while the temperature reaches its maximum potential, particularly when compared to the absorbing-emitting gas. This distinction becomes more pronounced when the opacity of the medium is thin ($\tau \leq 1$). When the gas is transparent, the radiation exchange among the cavity walls imposes a stratified temperature distribution on the adiabatic walls. The temperature and flow fields are asymmetrical, but considering the effects of volume radiation (absorbing-emitting), the temperature difference increases near the cold active wall. The cooling of the upper wall and the heating of the lower wall induce a homogenization of the gas temperature and a strong deformation of the thermal stratification at the heart of the cavity. The physical mechanism is different from the case of the transparent medium, since radiative gas-gas and gas-wall transfers have a direct effect on the temperature of the gas. The temperature of the side and horizontal walls is now imposed by the gas, the conductive flux being zero on these walls. Thus, compared to the scenario involving the transparent medium, the upper wall is cooled, the lower wall is heated.

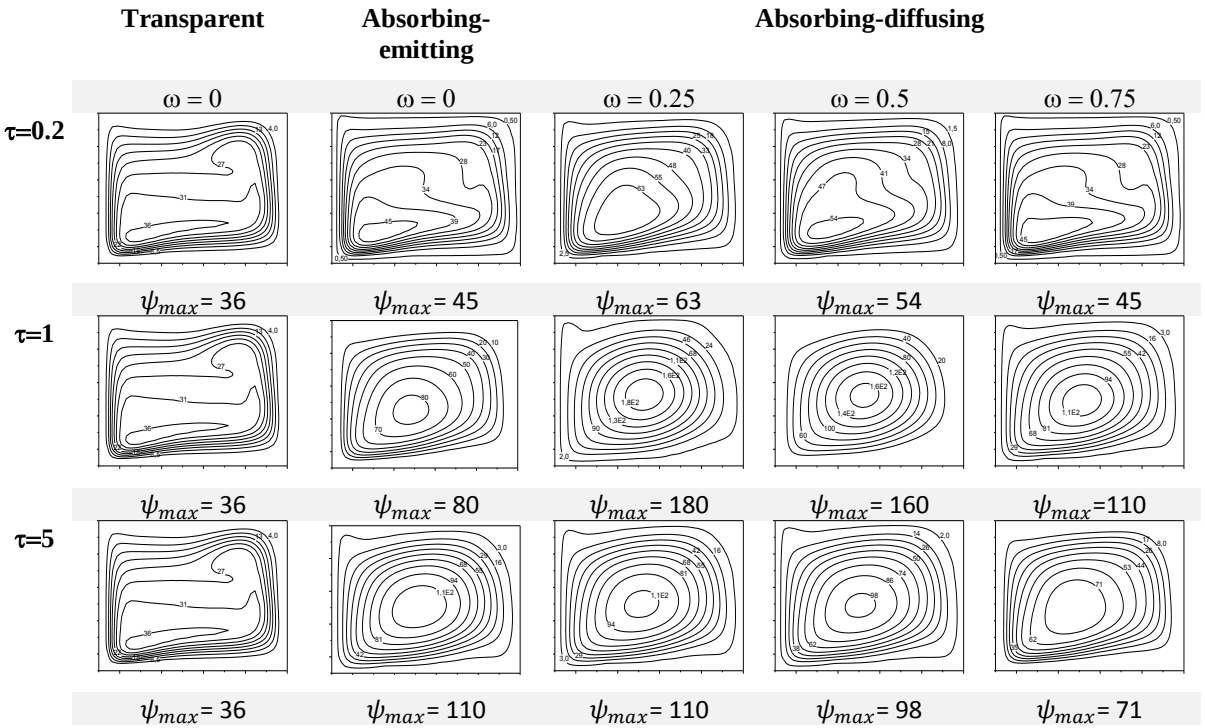

Figure 4. Streamlines for different media for Ra = 5.10^6 and Pr = 0.71

When the opacity is high, the coupling phenomenon is more sensitive to the absorbing-emitting medium, as its temperature is the most affected. Conversely, when the optical thickness is low, it becomes more sensitive to the absorbing-diffusing medium, as its temperature is the most affected. Additionally, a high value of the optical thickness significantly reduces the effect of the albedo coefficient. For a larger value of τ we observe a great temperature gradient close to the limit layer of the cold wall. Increased opacity of the medium results in a heightened radiation effect (figure 5). If the gas is viscous, the streamlines will retain their initial form. As the frequency ω grows, the impact of radiation diminishes, and the isotherms become the same when the opacity is very high (τ = 5). Opacity levels below 1 result in noticeable distortion.

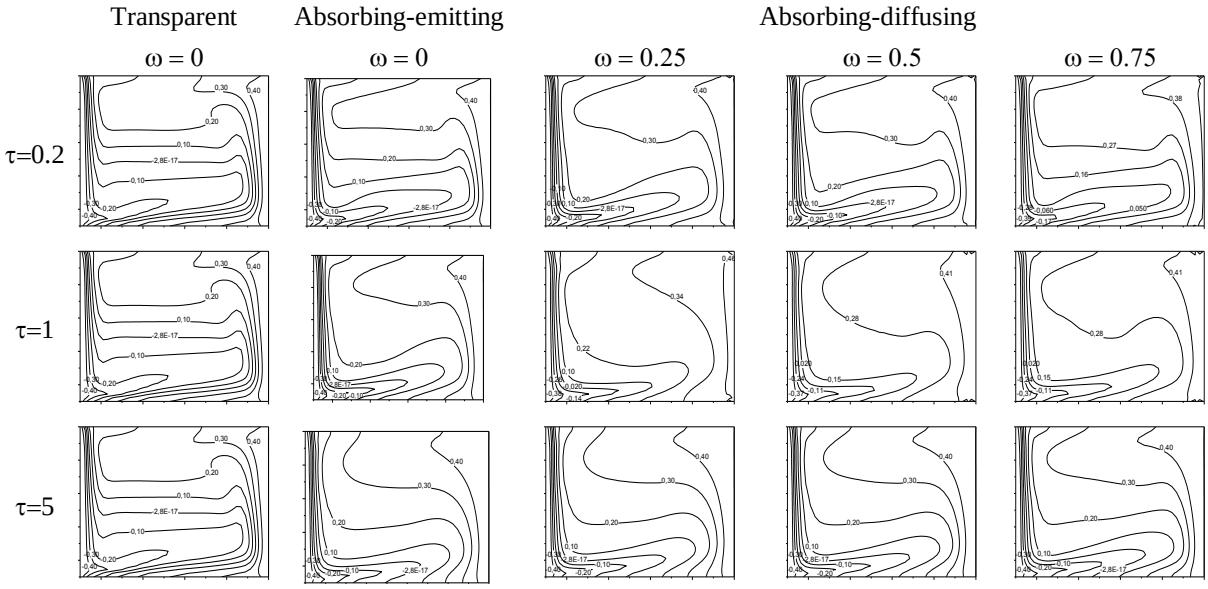

Figure 5. Isotherms for different mediums for Ra = 5.10^6 and Pr = 0.71

For the participating medium and in radiation presence, the cavity nucleus is warmer in contrast to the transparent medium case, which produces a significant alteration of the temperature gradient close to the left wall. Simultaneously, the isotherms stratification is broken, and the streamlines show a unicellular structure (figures 4 and 5). We notice that the cavity nucleus is more stratified when the medium becomes transparent (figure 5). The temperature distributions along the central axes for varying opacity levels and in the three

configurations, presented in figure 6, show that the thermal gradients undergo significant variations from one medium to another and increase with the increase in the albedo coefficient. However, we find almost the same temperature profile when the medium is more opaque.

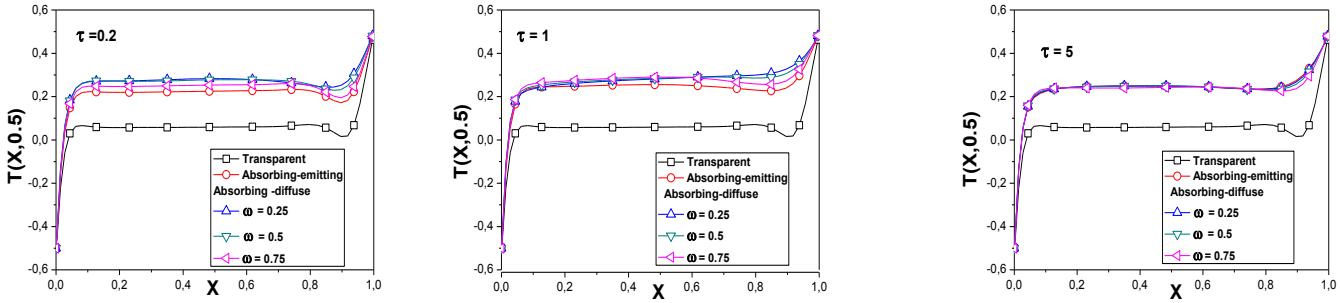

(a) (b) (c)

Figure 6. Temperature profiles at mid-height for Ra = 5.10^6 and Pl = 0.02, (a) τ =0.2, (b) τ =1, (c) τ =5.

The profiles of velocity components in the horizontal and vertical directions are shown in figures 7 and 8. Analysis of the data shows that optical thickness has a considerable influence on the maximum velocities (both horizontal and vertical) at the boundary layers of all three media. It can be seen that maximal velocity values increase with the optical thickness when $\tau \leq 1$and decrease when we increase the albedo coefficient. If $\tau = 5$ the maximal values decrease in comparison with a thinner medium ($\tau = 1$). Energy transfers between the gas and the walls can occur over long distances, allowing the fluid to move away from the walls. The volume of fluid flowing in the cavity becomes larger, which explains the boundary layers expanding and the velocities increasing. We deduce from the comparison between the three media studied that there is less radiation absorption in the case of the absorbing-emitting medium when the opacity is low (figure 10). With regard to the case where the gas is transparent, the thickening of the boundary layers is explained by the preheating of the gas along the lower wall, upstream of the ascending vertical boundary layer, and reciprocally by the cooling of the gas along the wall high. The circulation of the gas is clearly enhanced when the gas radiates. The cavity core is set in motion while it remains almost motionless in the case of the transparent medium. In terms of heat transfer, the variations of the average Nusselt numbers in the three media as a function of τ and ω, show that the absorbing-diffusing medium gives the best heat transfer when the medium is thin (table 4).

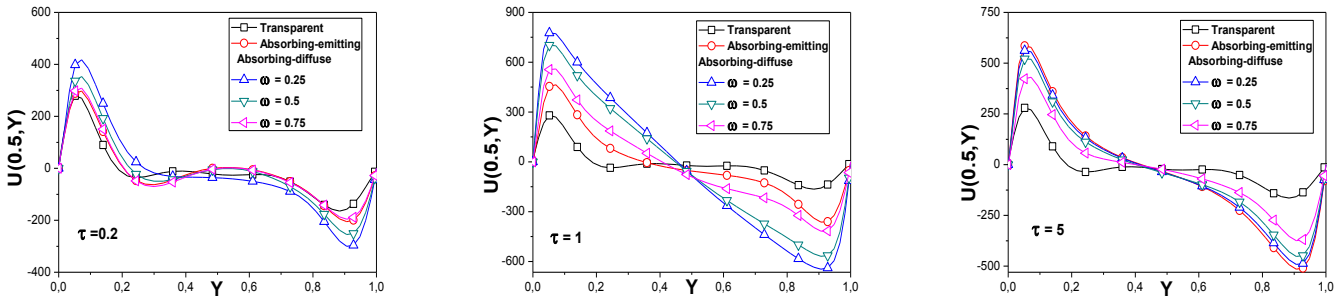

(a) (b) (c)

Figure 7. Horizontal velocity at vertical cross-section for Ra = 5.10^6 and Pl = 0.02 (a) τ=0.2, (b) τ =1, (c) τ =5

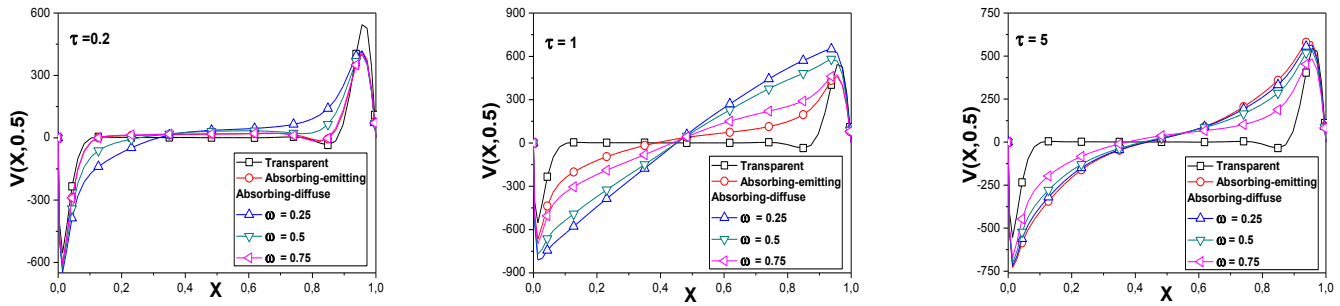

(a) (b) (c)

Figure 8. Vertical velocity at horizontal cross-section at Ra = 5.106 and Pl = 0.02
(a) τ =0.2, (b) τ =1, (c) τ =5

An additional objective of this study is to compare the behavior of the three media and their effects on heat exchanges in the non-Boussinesq (non-BC). The results show that there is a different behavior for heat

transfer distribution when the fluid changes. The average and local Nusselt number variations (convective, radiative and global) as a function of the albedo coefficient and the optical thickness appear in table 4 and in figures 9-11. When the medium is transparent and $\tau = 5$, the radiation notably enhances the heat flux, the contribution of convective and total Nusselt remains almost similar with small difference for the absorbing-emitting and diffuse media.

Table 4. Average convective, radiative, and total Nusselt numbers as function of τ and ω

	ω	τ	Nu_c	Nu_r	Nu_T
Transparent	0	0	9.807	49.425	58.055
Absorbing-emitting	0	0.2	7.236	46.379	52.511
		1	5.858	37.959	42.914
		5	5.733	28.037	33.77
absorbing-diffusing	0.25	0.2	5.988	173.644	179.632
		1	6.687	134.594	141.281
		5	5.392	27.522	32.914
	0.5	0.2	6.024	173.246	179.27
		1	7.108	133.977	141.085
		5	5.071	26.607	31.677
	0.75	0.2	6.829	172.739	179.568
		1	6.641	132.565	139.206
		5	4.983	24.624	29.607

For $\tau = 5$, and when the medium is transparent, radiation significantly increases the thermal flux. Simultaneously, the heat transfer in relation to convective and total Nusselt numbers is almost the same in both the absorbing-emitting and absorbing-diffusing media. Consequently, the transparent medium ($\tau = 0$) give a maximum heat transfer with respect to the participation of the medium. For the participating media, the absorbing-diffuse medium gives the best heat exchange. The albedo factor and optical depth decrease the radiative and global heat exchange. We can see that when the optical thickness is constant; the radiative and global Nusselt numbers increase with the albedo rise and inversely for the convective Nusselt (figures 9-11). Moreover, when the albedo is constant, the rates of heat exchange decrease with the optical thickness rise. The transparent medium always gives the best convective exchange. If the optical thickness is low ($\tau \leq 1$) the absorbing diffusing medium gives the best heat exchange. At $\tau = 5$, the participating medium emits less radiative flux compared to the non-participating medium. The decrease in temperature is attributed to the decline in radiative heat transfer over the heated surface with the increase in optical thickness. Radiative heat transfer occurs between the hot wall and an effective plane that maintains a higher temperature compared to the cold wall. We must notice that the radiative flux at the two cavity extremities is more important for the transparent medium when $\tau = 5$. When the gas opacity increases, this effect is near to disappear. When the medium is thin the absorbing-diffusing gas increases the radiative flow compared to the absorbing-emitting gas and there is a slight difference between the two mediums when the opacity is stronger.

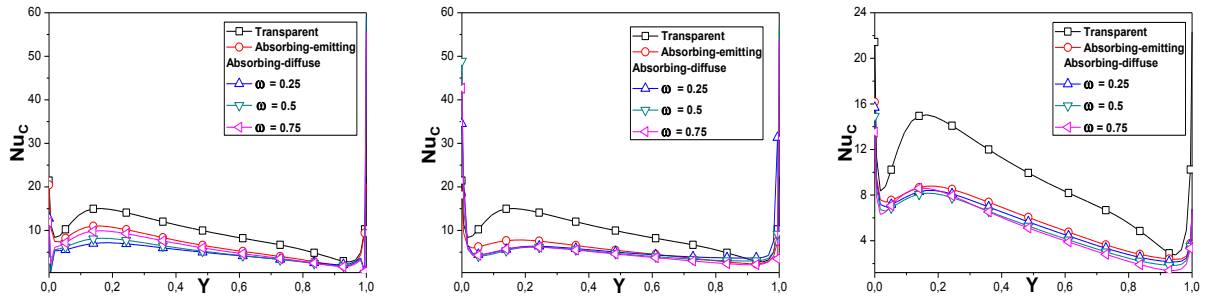

(a) (b) (c)

Figure 9. Profiles of local convective Nusselt number for Ra = 5.10^6 and Pl = 0.02
(a) τ = 0.2, (b) τ=1, (c) τ =5

The radiative power is represented in figure 12. The power fields of the two media are almost similar and the distribution is closer on the walls. The absorbing-emitting medium gives a better distribution of the radiative power than the absorbing-diffusing medium. The maximal values of the radiative power increase with the rise of the optical thickness and decrease with the albedo coefficient rise, which shows the absorbing quantity has played an important role on the radiative flow distribution compared to the diffuse quantity. The maximal values of the radiative power increase with the rise of the optical thickness and decrease with the increase in the albedo

coefficient, which shows the absorbing quantity has played an important role on the radiative flux distribution compared to the diffusing quantity.

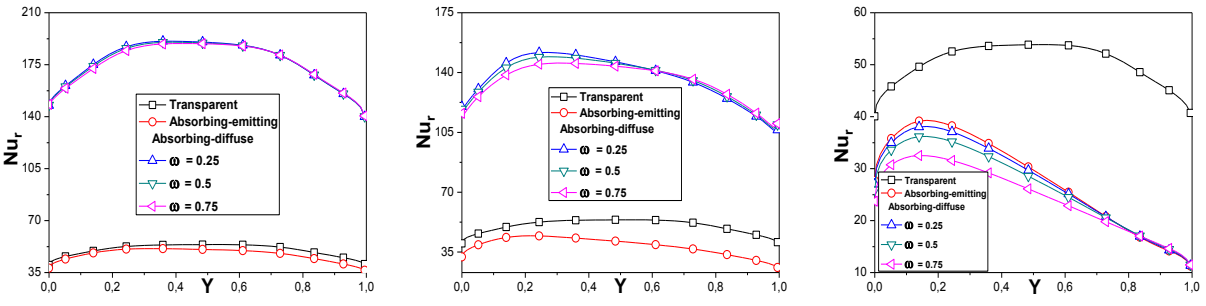

(a) (b) (c)

Figure 10. Profiles of local radiative Nusselt number for Ra = 5.10^6 and Pl = 0.02
(a) τ = 0.2, (b) τ=1, (c) τ =5

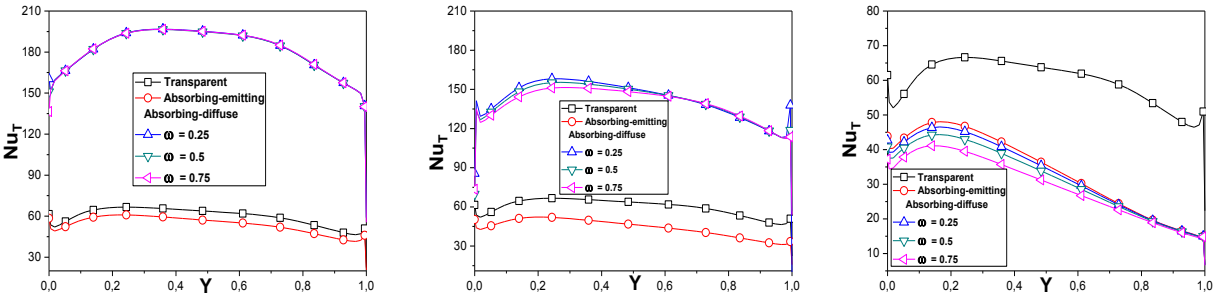

(a) (b) (c)

Figure 11. Profiles of local global Nusselt number for Ra = 5.10^6 and Pl = 0.02, (a) τ =0.2, (b) τ =1, (c) τ =5

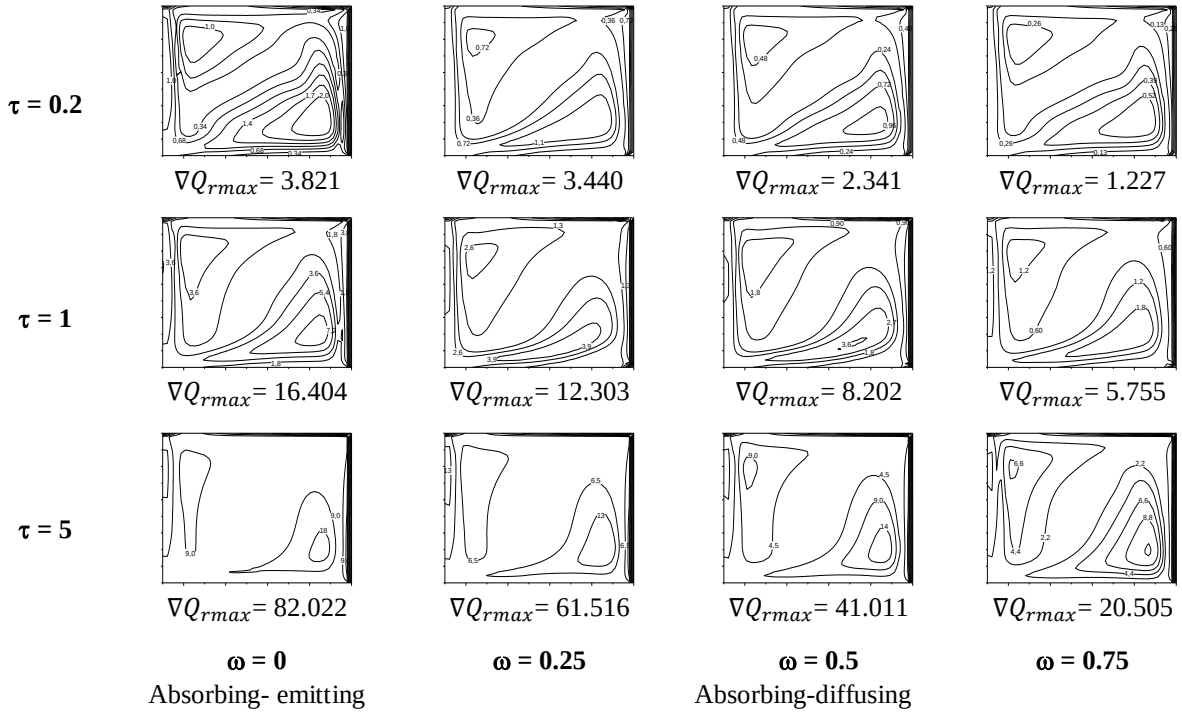

Figure 12. Radiative power for different values of the optical thickness in non-Boussinesq flow

In conclusion of our analyses, it is crucial to examine the impact of the intricate interactions observed in participating media. As discussed earlier, the interaction between gas molecules and the walls, along with gas-gas and gas-wall exchanges, significantly affects the temperatures of the walls. Typically, the upper wall cools, while the lower wall heats up, which is a clear deviation from the behavior observed in transparent media. The

effects of optical thickness further complicate these interactions. In thinner media, radiative heat transfer remains highly efficient, with the absorbing-diffusing medium showing superior performance compared to an absorbing-emitting one. The absorption and scattering of radiation stimulate fluid motion, which enhances convective heat transfer. In contrast, thicker media exhibit increased opacity, leading to a reduction in radiative flux, thereby weakening convective heat transfer. In such cases, conduction and localized radiation exchanges become the dominant modes of thermal transfer.

8. Conclusion

Natural convection combined with volumetric radiation within an enclosure containing an absorbing, emitting, and isotropically scattering gray medium under normal surrounding conditions was studied. Solutions of coupled conservation equations of continuity, momentum, and heat were obtained using the finite volume method (FVM) with Simpler algorithm. The radiative transfer equation was angularly discretized by the discrete ordinates method to calculate the radiative heat source term in the energy equation. The developed numerical code was checked by comparison with the bibliography results. The heat transfer and the dynamics of the fluid were examined and analyzed in three different media and by varying the albedo of the diffusion in a range between 0 and 0.75 for different optical thicknesses. According to the obtained results, we can say that the LMN model approximation highly overestimates the radiative transfer gas to gas and to walls: The radiative power maximum is higher for the absorbing-emitting case. From the results obtained, it was noted that the LMN model approximation strongly overestimates the radiative transfer gas to the gas and to the walls:

- The maximum radiative power is higher for the absorbing-emitting case. The transparent medium has given a maximal heat transfer ($\tau = 5$). For participating gases, the absorbing-diffusing medium is more effective under the LMN approximation when the opacity is low.
- The flow is more intense, and the maximum vertical velocity is higher. In the cavity center, the isotherms are not horizontal because of the large deformation.
- For high opacity (τ=5), the heat transfer through the cavity is higher for transparent medium. Lower velocity magnitudes are observed when the medium is more diffusing, characterized by a higher albedo coefficient. The influence of albedo diffusion is particularly significant in flows with thin optical thickness.

This study provides valuable insights into natural convection and radiation in gray media, but its limitations include simplified assumptions. The use of a single geometry restricts its applicability. Future research should incorporate anisotropic effects, explore various conditions, and consider different geometries, such as inclined and trapezoidal shapes, for broader relevance.

Nomenclature

Cp, Cv	specific heat capacities [J. kg $^{-1}$. K^{-1}]	Q_r	dimensionless radiative heat flux $Q_r = Hq_r/k(T_H - T_C)$
G	gravitational acceleration [m.s^{-2}]	q_{rinc}	incident radiative flux (W. m^{-2})
k	thermal conductivity[W m^{-1} K^{-1}]	Q_{rinc}	dimensionless incident radiative flux, $Q_{rinc} = \frac{q_{rinc}}{\sigma T_0^4}$
L	dimensionless radiation intensity $L = \frac{L'}{\sigma T_0^4}$	r	ideal gas constant $r = (C_p - C_v)$[J. kg $^{-1}$. K^{-1}]
L_b	radiation intensity of the black body [W.m^{-2}]	Ra	Rayleigh number $Ra = \frac{2\varepsilon_b \rho_0 g H^3}{\mu_0 \alpha_0}$
H	dimension of the enclosure [m]	T	dimensionless temperature $T = \frac{T' - T_0}{\Delta T}$
Nu	average Nusselt number	T_0	reference temperature $T_0 = \frac{T_H + T_C}{2}$ [K]
$\bar{P}$	mean thermodynamic pressure $\bar{P} = \frac{\bar{p}}{P_0}$	t	dimensionless time $t = \frac{t' \alpha_0}{H^2}$
P_0	reference pressure $P_0 = \rho_0 r T_0$	u, v	dimensional velocity-components [m.s^{-1}]
Pr	Prandtl number $Pr = \frac{\mu_0}{\rho_0 \alpha_0}$	U, V	dimensionless velocity-component $U = \frac{u}{\alpha_0/H}$, $V = \frac{v}{\alpha_0/H}$
Pl	Planck number $Pl = \frac{\Delta T k_0}{H \sigma T_0^4}$	X, Y	dimensionless coordinates $X = \frac{x}{H}$, $Y = \frac{y}{H}$

q_r	radiative heat flux [W. m^{-2}]	x, y	Cartesian coordinates [m]

Greek symbols

α	thermal diffusivity, $\alpha = k/\rho.Cp$[m^2.s^{-1}]	ρ	fluid density, kg m^{-3}
ε	emissivity	σ	Stefan-Boltzmann constant [W m^{-2} K^{-4}]
ε_b	Boussinesq parameter$\varepsilon_b = \frac{\Delta T}{2T_0}$	$\overrightarrow{\Omega}$	direction vector, $\vec{\Omega} = \xi\vec{\imath} + \eta\vec{\jmath}$
κ	absorption coefficient [m^{-1}]	τ	optical thickness, $\tau = \kappa H$
μ	Dynamic viscosity, [Pa.s]	ΔT	temperature difference, $\Delta T = T_H - T_C$
ξ, η	direction cosines	π	dimensionless pressure, $\pi = \frac{P - \bar{P} + \rho_0 gz}{\rho_0 V_0^2}$
ω	albedo coefficient	γ	Thermodynamic ratio $\gamma = \frac{C_p}{C_v}$
ω_m	weight in the direction Ω_m		

Subscripts

‘	dimensional variables	*0*	reference state
BS	Boussinesq model	*C*	cold
R	Radiative	*H*	hot
CV	Convective	*T*	total

References

[1] G. Lauriat, Combined Radiation–Convection in Gray Fluids Enclosed in Vertical Cavities, J. Heat Transfer, 104 (1982), 4, pp. 609 - 615

[2] A. Yucel, S. Acharya , ML. Williams , Natural Convection and Radiation in a Square Enclosure , Numer. Heat Tr. A- Appl., 15 (1989), 2, pp. 261 – 278.

[3] A. Draoui, F. Allard, C. Beghein, Numerical Analysis of Heat Transfer by Natural Convection and Radiation in Participating Fluids Enclosed in Square Cavities , Numer. Heat Tr. A - Appl., 20 (1991), 2, pp. 253 -261

[4] T. Fusegi , B. Farouk, Laminar and Turbulent Natural Convection - Radiation Interactions in a Square Enclosure Filled with a Non gray Gas, Numer. Heat Tr. A - Appl., 15 (1989), 3, pp. 303 - 322

[5] Z. Tan , J.R. Howell , Combined Radiation and Convection in a Two – Dimensional Participating Square Medium , Int. J. Heat Mass Transfer, 34 (1991), 3, pp. 785 - 793

[6] M.N. Borjini , H. Ben Aissia, K. Halouani, B. Zghmati , Effect of Radiative Heat Transfer on the Three – Dimensional Buoyancy Flow in Cubic Enclosure Heated from the Side , Int. J. Heat Fluid Flow, 29 (2008), pp. 107 - 118.

[7] G. Colomer, R. Consul, A. Oliva, Coupled Radiation and Natural Convection. Different Approaches of the SLW Model for a Non - Gray Gas Mixture , J. Quant. Spectrosc. Radiat. Transf., 107 (2007), pp. 30 – 46.

[8] K. Lari , M. Baneshi, S.A. Gandjalikhan Nassab, A. Komiya, S. Maruyama , Numercial Study of Non – Gray Radiation and Natural Convection Using the Full - Spectrum K - Distribution Method , Numer. Heat Tr. A – Appl., 61 (2012), p. 61 – 84.

[9] R. Capdevila , O. Lehmkuhl,F.X. Trias, C.D. Pérez-Segarra, G. Colomer , Turbulent Natural Convection in a Differentially Heated Cavity of Aspect Ratio 5 Filled with Non – Participating and Participating Grey Media , J. Phys. Conf. Ser. (2011), 318, 042048.

[10] F. Moufekkir, M.A. Moussaoui, A. Mezrhab, H. Naji, D. Lemonnier, Numerical Prediction of Heat T ransfer by Natural Convection and Radiation in an Enclosure Filled with an Isotropic Scattering Medium, J. Quant. Spectrosc. Radiat. Transf., 113 (2012), 13, pp. 1689 – 1704.

[11] X. Liu , G. Gong, H. Cheng , Combined Natural Convection and Radiation Heat Transfer of Various Absorbant – Emitting - Scattering Media in a Square Cavity , Adv. Mech. Eng., 2014 (2014), 403690, pp.1-10.

[12] A. Mezrhab , D. Lemonnier, S. Meftah, A. Benbrik, Numerical Study of Double - Diffusion Convection Coupled to Radiation in a Square Cavity Filled with a Participating Grey Gas , J. Phys. D: Appl. Phys., 41 (2008), 19, pp. 1-16.

[13] K. H. Byun , K . H. , M. HyukIm , Radiation Laminar Free Convection in a Square Duct with Specular by Absorbing – Emitting Medium, KSMEI Int. J., 16 (2002), 10, pp. 1346-1354

[14] R. Chaabane , F. Askri, A. Jemni, S. Ben Nasrallah, Numerical Study of Transient Convection with Volumetric Radiation Using an Hybrid Lattice Boltzmann B G K - Control Volume Finite Element Method, J. Heat Transfer, 139 (2017), 9, pp. 1-7.

[15] H. Wang , S. Xin, P. Le Quéré , Numerical Study of Natural Convection – Surface Radiation Coupling in Air – Filled Square Cavities, C . R. Mec ., 334 (2006) , 1 , pp. 48 – 57.

[16] S. Hamimid , M. Guellal , M. Bouafia, Numerical Simulation of Combined Natural Convection Surface Radiation for Large Temperature Gradients , J. Thermophys. Heat Transfer , 29 (2015) , 3 , pp . 1509 – 1517.

[17] M. Bouafia , et al. , Non - Boussinesq Convection in a Square Cavity with Surface Thermal Radiation, Int . J. Therm. Sci., 96 (2015), pp. 236 – 247.

[18] T. Kogawa, J. Okajima, A. Komiya, S. Maruyama, Effect of Gas Radiation-Depended Natural Convection on the Transition of Spatially Developing Boundary Layers, Int. J. Heat Mass Transf., 177 (2021), pp. 121580.

[19] S. Parsaee, S. Payan, A. Payan, Semi-Transient Thermal Analysis from MHD-Participating Fluid into a Square Cavity with Variable Optical Thickness, Int. J. Therm. Sci., 169 (2021), pp. 107072.

[20] E. G. Barbosa, M. E. V. Araujo, M. A. Martins, E.G. Barbosa, Natural Convection and Radiation in Enclosures with Semi-transparent Medium: Conjugate CFD Analysis, J. Appl. Fluid Mech., 15 (2022), 5, pp. 1307-1318.

[21] H. Sertel , Z. Altaç, Numerical Investigation of Combined Effects of Radiation and Convection Heat Transfer from Tube Banks Placed in a Participating Medium, Numer. Heat Transf. A, 85 (2024), pp.1191-1217.

[22] F. E. Moutahir , Y. Belhamadia , M. Seaid , M. El-Amrani , Modelling and Simulation of Radiative Heat Transfer in Non-Grey Absorbing and Emitting Media Under Phase Change, Comput. Math. Appl., 176 (2024), pp. 432-446.

[23] N. Rachedi , M. Bouafia, M. Guellal, S. Hamimid, Effect of Radiation on the Flow Structure and Heat Transfer in a 2 - D Gray Medium , Thermal Science , 23 (2019) , 6 A , pp. 3603 – 3614.

[24] M.F. Modest, Radiative Heat Transfer , 2nd ed. , Academic Press , Sandiego, U. S. A., 2003.
[25] J.C. Chai , A Finite Volume Method for Radiation Heat Transfer, Ph . D. Thesis, University of Minnesota, U.S.A., 1994.

[26] S.V. Patankar, Numerical Heat Transfer and Fluid Flow, Mc-Graw-Hill , New-York, U.S.A., 1980.

[27] W. A. Fiveland, Three – Dimensional Radiative Heat Transfer Solutions by the Discrete Ordinates Method , J . Thermophys Heat Transf. , 2 (1988) , 4 , pp. 309 – 316.

[28] M.M. Razzaque , D.E. Klein, J.R. Howell, Finite Element Solution of Radiative Heat Transfer in a Two - Dimensional Rectangular Enclosure with Gray Participating Media , J. Heat Transfer, 105 (1983),4 , pp. 933 – 936.

[29] S. Laouar Meftah, , Modeling of Natural Double Diffusion Convection in Mixture Gases Absorbing and Emitting Radiation (in French) , Ph. D. Thesis, University of Boumerdes , Algeria, 2010.

Received: 5.10.2024.
Revised: 18.12.2024.
Accepted: 8.1.2025.